Irreversible Thermal Denaturation of β-Hemocyanin of *Helix pomatia* and its Substructures Studied by Differential Scanning Calorimetry

Krassimira Idakieva[a], Constant Gielens[b], Nurul I. Siddiqui[b], Lyubka Doumanova[c], Boyka Vasseva[a], Georgi Kostov[d], and Valery L. Shnyrov[e]

[a] Institute of Organic Chemistry, Bulgarian Academy of Sciences, Acad. G. Bonchev-Str. Bl. 9, 1113 Sofia, Bulgaria
[b] Laboratory of Biochemistry, Chemistry Department, Katholieke Universiteit Leuven, Celestijnenlaan 200 G, 3001 Leuven-Heverlee, Belgium
[c] Institute of Microbiology, Bulgarian Academy of Sciences, 1113 Sofia, Bulgaria
[d] Institute of Biophysics, Bulgarian Academy of Sciences, 1113 Sofia, Bulgaria
[e] Department of Biochemistry and Molecular Biology, Universidad de Salamanca, 37007 Salamanca, Spain

Reprint requests to Prof. K. I. or Prof. V. L. S.; E-mail: idakieva@orgchm.bas.bg or shnyrov@usal.es

Z. Naturforsch. **62a,** 499 – 506 (2007); received April 4, 2007

The thermal denaturation of β-hemocyanin from the gastropod *Helix pomatia* (β-HpH) at neutral pH was studied by means of differential scanning calorimetry (DSC). The denaturation was completely irreversible as judged by the absence of any endotherm on rescanning previously scanned samples. Two transitions, with apparent transition temperatures (T_m) of ca. 84 °C (main transition) and ca. 88 °C (minor transition), were detected by DSC in 20 mM MOPS buffer, containing 0.1 M NaCl, 5 mM $CaCl_2$ and 5 mM $MgCl_2$ at pH 7.2 (buffer A), using a heating rate of 1.0 K min^{-1}. Both T_m values were dependent on the scanning rate, suggesting that the thermal denaturation of β-HpH is a kinetically controlled process. The T_m and specific enthalpy values (ΔH_{cal}) for the thermal denaturation of β-HpH were found to be independent of the protein concentration, indicating that the dissociation of the protein into monomers does not take place before the rate-determining step of the process of thermal unfolding started. A successive annealing procedure was applied to obtain the experimental deconvolution of the irreversible thermal transitions. These transitions are tentatively attributed to the denaturation of, respectively, the wall (main transition) and the collar of the β-HpH molecule. The activation energies (E_A) of both transitions were found to be similar (about 500 kJ mol^{-1}).

In 130 mM glycine/NaOH buffer, pH 9.6 (buffer B), with β-HpH dissociated into subunits, the calorimetric profile had a more complex character. This could be ascribed to a different stability of the functional units (FUs) constituting the β-HpH subunit. FU *d*, which in the cylindrical didecameric β-HpH molecule is located in the wall, was markedly less stable than FU *g*, which belongs to the collar. The thermal denaturation of FUs *d* and *g* was described by the two-state irreversible model. On the basis of this model, the parameters of the Arrhenius equation were calculated.

Key words: Hemocyanin; *Helix pomatia*; Thermal Stability.

1. Introduction

Hemocyanins (Hcs) are oligomeric copper-containing respiratory proteins, freely dissolved in the hemolymph of many arthropod and mollusc species. The hemocyanin molecule in molluscs has the shape of a hollow cylinder (35 nm in diameter) [1] and is constituted of ten (cephalopods) or twenty (gastropods) subunits with a molecular mass of 350 – 450 kDa. In gastropodan Hcs, the quaternary structure (didecamer with a molecular mass of ∼ 9 MDa and a cylinder height of 38 nm [1]) consists of two axially assembled decamers. The gastropodan Hc subunit itself is subdivided into eight functional units (FUs) of approximately 50 kDa denoted *abcdefgh*, each containing a single dioxygen binding site [2, 3]. FUs *abcdef* make up the wall of the Hc cylinder, while FUs *g* and *h* form the collar. The globular FUs are more protease-resistant than the

Abbreviations: DSC, differential scanning calorimetry; Hc, hemocyanin; β-HpH, β-hemocyanin of *Helix pomatia*; RtH, *Rapana thomasiana* hemocyanin; FU, functional unit; MOPS, 3-[*N*-morpholino]-propanesulfonic acid.

intervening or "linker" regions, allowing their isolation.

Although the structure and function of the Hcs have been investigated in depth, only a few studies have addressed the thermostability of these dioxygen carriers [4–6]. Recently, using differential scanning calorimetry (DSC) we reported for the first time an investigation on the thermostability of a molluscan Hc, namely that of the marine gastropod *Rapana thomasiana* (referred to as RtH) [7].

The Hc of the gastropod mollusc *Helix pomatia* (vineyard snail) consists of three components. Next to two α-components (α_D- and α_N-Hc) there is also a β-component (referred here to as β-HpH) [2]. The latter differs from the α-Hcs in its ability to precipitate or crystallize during dialysis against sodium acetate buffer, pH 5.3, at low ionic strength (10 mM), and in the subunit composition, which consists of only one type of polypeptide chain (β subunits) as compared with two types (the α and α' subunits) in each of the two α-Hcs [8]. Owing to this subunit homogeneity, structural investigations have mainly been performed on β-HpH [9]. The eight FUs constituting the structural subunit of β-HpH have been isolated [10]. The primary structure of the FUs *d* [11] and *g* [12] has been obtained through amino acid sequencing.

Differential scanning calorimetry is a powerful technique for characterizing temperature-induced conformational changes in proteins. Equilibrium analyses of DSC thermograms corresponding to reversible unfolding of proteins provides information about the thermodynamics and mechanisms of the reversible unfolding [13, 14]. However, the thermal denaturation of many proteins is irreversible due to some alteration, such as autolysis, aggregation, or chemical alteration of residues [15], that locks the protein in a final state, after which it is unable to fold back to the native structure. In such cases, kinetic models are applied for analyzing the heat capacity curves to check whether the model-derived DSC transitions are dependent on the DSC scan rate or not [16–19].

In this work, by means of high-sensitivity DSC, we studied the thermal denaturation of the *Helix pomatia* β-Hc both in its associated form, i. e. at neutral pH when it is present as a didecamer of 450 kDa subunits, and in its dissociated form, i. e. at alkaline pH when it is present as monomeric subunits. For comparison, the thermostability of FUs *d* and *g*, which are located in different parts of the cylindrical didecameric molecule, was also investigated.

2. Materials and Methods

2.1. Protein Sample Preparation

HpH (total) was isolated from the hemolymph of the terrestrial snails *Helix pomatia*. The HpH was solubilized in 0.1 M sodium acetate buffer, pH 5.7, and the β-HpH precipitated by dialysis against 0.01 M sodium acetate buffer, pH 5.3, as described elsewhere [10]. Then β-HpH was solubilized in 0.1 M sodium phosphate buffer, pH 6.5, at a concentration of 10–40 mg/ml (stock solution). FUs Hc *d* and Hc *g* were isolated after limited trypsinolysis of β-HpH subunits [11, 12]. The purity of the FUs was checked by SDS-PAGE.

The buffer conditions used to study the β-HpH in either the associated (didecameric Hc) or dissociated state (subunits) were chosen on the basis of the pH stability region of β-HpH [20] and the buffer dependence of the DSC measurements of *Rapana thomasiana* Hc [7]. Accordingly, the calorimetric experiments were carried out in 20 mM MOPS buffer, containing 0.1 M NaCl, 5 mM $CaCl_2$ and 5 mM $MgCl_2$ at pH 7.2 (20 °C) (buffer A) for the didecameric β-HpH, and in 130 mM glycine/NaOH buffer, pH 9.6 (20 °C) (buffer B) for the β-HpH subunits. The protein samples were dialyzed extensively against the buffer used in the scanning experiment. After dialysis, the protein concentration was determined spectrophotometrically using the absorption coefficient $A_{278}^{0.1\%} = 1.416\ \mathrm{ml\,mg^{-1}\,cm^{-1}}$ for the β-HpH and the subunits, $1.277\ \mathrm{ml\,mg^{-1}\,cm^{-1}}$ for the FU Hc *d* and $1.233\ \mathrm{ml\,mg^{-1}\,cm^{-1}}$ for the FU Hc *g* [21].

2.2. Differential Scanning Calorimetry

Calorimetric measurements were performed on a DASM-4 (Biopribor, Pushchino, Russia) high-sensitivity differential scanning microcalorimeter, with a sensitivity greater than $0.017\ \mathrm{mJ\,K^{-1}}$ and a noise level less than $\pm 0.05\ \mu$W. A constant pressure of 2 atm was maintained throughout the DSC experiments to prevent possible degassing of the solution on heating. Each sample run was preceded by a base line run with buffer-filled cells. The protein solution in the calorimetric cell was reheated after cooling from the first run to estimate the reversibility of the thermally induced transitions. In all cases, the thermal denaturation was found to be irreversible, and therefore the thermogram corresponding to the reheating run was used as the in-

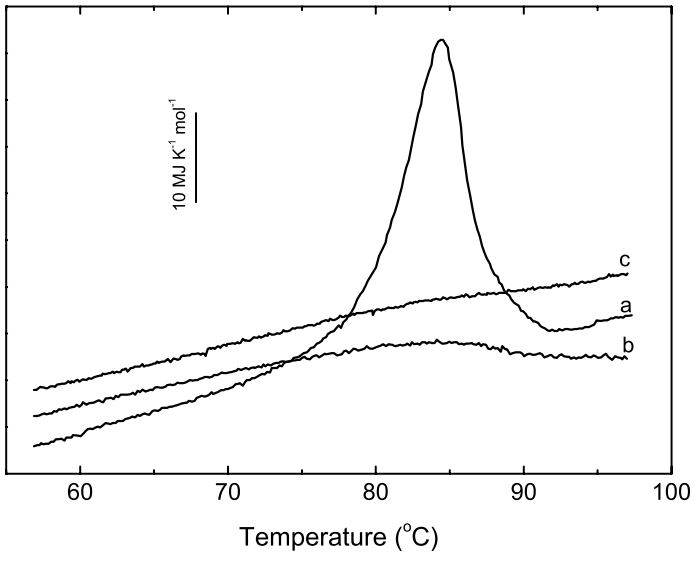

Fig. 1. (a) Original calorimetric recording of the apparent heat capacity of β-HpH as a function of the temperature. (b) Reheating scan. (c) Base line obtained with buffer in both cells of the calorimeter; the experimental curve shown is for 4 mg/ml β-HpH in buffer A at a scan rate of 1 K min^{-1}.

strumental base line. The transitions were corrected for the difference in heat capacity between the initial and final state using the chemical base line, in accordance with [22]. The molar excess heat capacity curves, obtained by normalizing for the protein concentration and the known volume of the calorimetric cell, were smoothed and plotted using the Windows-based software package (Origin) supplied by MicroCal. The data were analyzed by non-linear least-squares fitting programs, as reported elsewhere [23]. In all cases the correlation coefficient (r), used as a criterion for the accuracy of fitting, was calculated according to

$$r = \sqrt{1 - \sum_{i=1}^{n} \left(y_i - y_i^{\text{calc}}\right)^2 / \sum_{i=1}^{n} \left(y_i - y_i^{\text{m}}\right)^2}, \qquad (1)$$

where y_i and y_i^{calc} are, respectively, the experimental and calculated values of the measurable parameter, y_i^{m} is the mean of the experimental values of the measurable parameter and n the number of points. In all fitting procedures r was not less than 0.99. In the calculation of the molar quantities, the molecular masses used for the β-HpH, its subunits, FU d and FU g were 9 MDa, 450 kDa, 50 kDa and 55 kDa, respectively.

DSC transitions were analyzed in terms of the two-state kinetic model:

$$\text{N} \xrightarrow{k} \text{D}, \qquad (2)$$

which is a limiting case of the Lumry-Eyring model [24]. This model considers only two significantly populated macroscopic states: the initial or native state (N), and the final or denatured state (D), the transition between which is determined by a strongly temperature-dependent first-order rate constant (k). In this case, the excess heat capacity C_p^{ex} is given by the following equation [23]:

$$C_p^{\text{ex}} = \frac{1}{\nu}\Delta H \exp\left\{\frac{E_{\text{A}}}{R}\left(\frac{1}{T^*} - \frac{1}{T}\right)\right\} \cdot \exp\left\{-\frac{1}{\nu}\int_{T_0}^{T} \exp\left[\frac{E_{\text{A}}}{R}\left(\frac{1}{T^*} - \frac{1}{T}\right)\right] \mathrm{d}T\right\}, \qquad (3)$$

where $\nu = \mathrm{d}T/\mathrm{d}t$ (K min^{-1}) is a scan rate value, ΔH the enthalpy difference between the denatured and native states, E_{A} the activation energy of the denaturation process, R the gas constant, and T^* the temperature where k is equal to 1 min^{-1}.

3. Results and Discussion

3.1. DSC Study of Associated β-HpH (Didecamers of Subunits)

The thermogram for β-HpH in buffer A, at a scanning rate of 1 K min^{-1}, is shown in Figure 1. Heat absorption is observed between 70 and 92 °C with an apparent transition temperature, T_{m}, at 84 °C (Fig. 1, line a). A second minor transition at ca. 88 °C can also be discerned in the thermogram. Judging from the absence of any transitions upon rescanning the

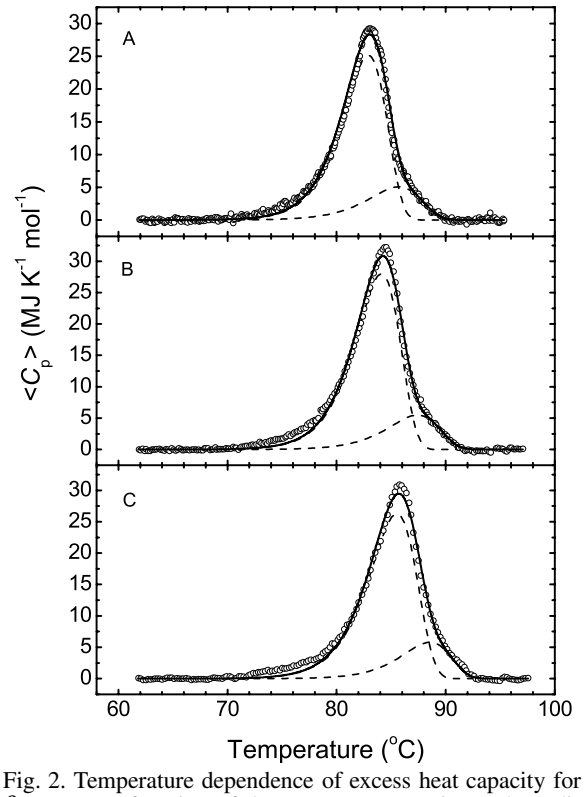

Fig. 2. Temperature dependence of excess heat capacity for β-HpH as a function of the scan rate. Experimental conditions as in Figure 1. Scan rates were 0.5 (A); 1.0 (B) and 2.0 K min^{-1} (C). Symbols show the experimental data and dashed lines show the result of the experimental deconvolution of the heat capacity curves into individual components with the successive annealing procedure (see text for details). Solid lines are the results of the superposition of the individual contours.

samples, the thermal denaturation of β-HpH is irreversible (Fig. 1, line b). Furthermore, the protein sample extracted from the calorimetric cell after a first scan showed visible turbidity. Irreversibility of the thermal denaturation was also observed in the DSC measurements of the Hc from the related gastropod *Rapana thomasiana* (RtH) [7] and is a common property of large Hc molecules due to aggregation after heating to denaturation temperatures.

From comparison with data of other Hcs it can be concluded that the thermostability of β-HpH is very similar to that of RtH (T_m = 83 °C; [7]). Also the specific calorimetric enthalpy ΔH_{cal} (190 MJ mol^{-1} or 21 J g^{-1}), calculated by the integration of the heat capacity curve, is very similar to that obtained by DSC measurements of RtH (184 MJ mol^{-1}; [7]). The Hc of the lobster *Palinurus vulgaris* (T_m = 63 °C; [4]) is much less heat-resistant compared to β-HpH, while the Hc from the tarantula *Eurypelma californicum* has extreme thermostability (T_m = 90 °C; [5]). Melting temperatures of 68 and 76 °C, respectively, have been determined from the temperature dependence of the ellipticity of the Hcs from the gastropods *Megathura crenulata* and *Haliotis tuberculata* [6].

Owing to the irreversibility of the thermal denaturation of β-HpH, thermodynamic parameters cannot be obtained because of the strong distortion of the DSC transitions due to the kinetics of the irreversible formation of the final state. Nevertheless, it is possible to obtain kinetic information from the analysis of the irreversible process. Figure 2 shows the corrected calorimetric traces, i. e. the excess specific heat capacity function vs. temperature profiles for β-HpH in buffer A at three different scan rates (0.5, 1.0 and 2.0 K min^{-1}). The transition temperature of the irreversible thermal denaturation of β-HpH is dependent on the scan rate: the maximum of the DSC profiles is shifted toward lower temperatures with a decrease in the heating rate, indicating that the process is kinetically controlled.

Since β-HpH is an oligomeric protein, thermally induced denaturation could be accompanied by dissociation into subunits. According to equilibrium thermodynamics, any change in the oligomerization state of the protein during the denaturation process should produce a concentration dependence of T_m [25]. The lack of such dependence may therefore be taken as evidence that the denatured protein remains in the same oligomerization state like the native protein [26]. This interpretation can also be applied to irreversible protein denaturation [27, 28]. The T_m and ΔH_{cal} values for the thermal denaturation of β-HpH in buffer A were found to be independent of the protein concentration within the 2.8 – 6.3 mg/ml range (data not shown). Also, in DSC studies of the thermal denaturation of the hemocyanins of *Palinurus vulgaris* [4] and *Rapana thomasiana* [7] no concentration dependence of T_m was observed.

As reported above, the thermal denaturation of β-HpH is irreversible. Therefore, analysis of DSC contours was attempted with a successive annealing procedure, which is useful for the experimental deconvolution of complicated completely or partially irreversible thermal transitions [29, 30]. The procedure used to assay the Hc was as follows: the Hc solution was heated at the scan rate 0.5 K min^{-1}. The first complete DSC scan (Fig. 3A, line a) afforded insight into the num-

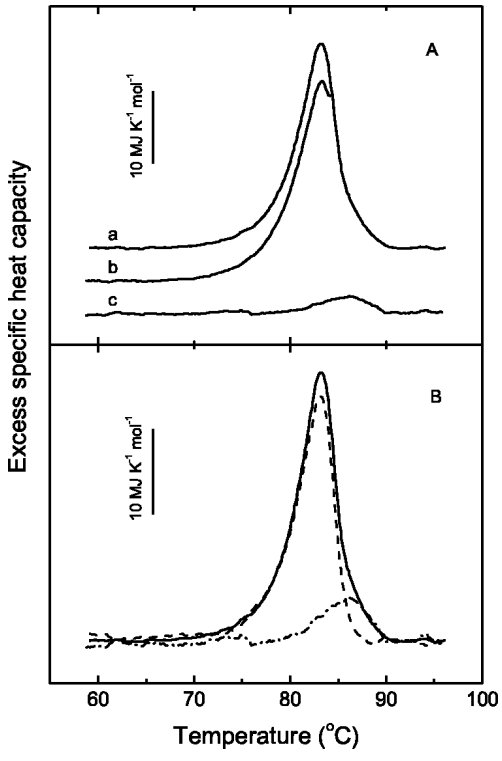

Fig. 3. Demonstration of the successive annealing procedure. (A) Calorimetric profile of β-HpH in buffer A at a heating rate of 0.5 K min^{-1} (line a). The first scan (line b), in accordance with this procedure, was stopped at 84 °C, the second one (line c) at 96 °C. The lines are displaced for clarity. (B) Result of deconvolution of the experimental contour (solid line), which provides two elementary contours (dashed and dashed-dotted lines). See text for details.

ber (two) and temperatures of the maxima of the elementary transitions (close to 83 and 86 °C). Then, a new protein solution of the same composition was placed in the measurement cell of the microcalorimeter and heated to 84 °C (Fig. 3A, line b). The sample was then cooled and heated again up to 96 °C (Fig. 3A, line c). In the latter case, we obtained the real contour of the second transition only with decreased intensity, which is the result of contour overlapping. Therefore, the final shape (Fig. 3B, dash-dotted line) of the second contour was obtained by multiplying on any of the coefficients in order to optimize the intensity of this transition in the zone where there were no overlapping elementary contours – in this case, at a temperature of 87.5 °C. Following this, the first elementary contour (Fig. 3B, dashed line) was obtained by subtracting the second elementary contour from the complete DSC scan (Fig. 3B, continuous line).

Table 1. Arrhenius equation parameter estimates for the two-state irreversible model of the thermal denaturation of β-HpH at pH 7.2.

		Temperature scan rate, K min^{-1}		
Transition	Parameter	0.5	1.0	2.0
First	ΔH, MJ mol^{-1}	135 ± 5	153 ± 7	153 ± 7
	T^*, °C	85.7 ± 0.2	85.5 ± 0.2	85.7 ± 0.2
	E_A, kJ mol^{-1}	528 ± 9	521 ± 7	501 ± 8
Second	ΔH, MJ mol^{-1}	33 ± 1	35 ± 1	35 ± 1
	T^*, °C	89.8 ± 0.2	89.5 ± 0.3	89.1 ± 0.3
	E_A, kJ mol^{-1}	443 ± 8	459 ± 8	470 ± 8

As is evident from Fig. 2, the DSC traces for the hemocyanin were strongly dependent on the scan rate, which prompted us to analyze this non-equilibrium process based on the simplest model of irreversible thermal denaturation of proteins (2). The excess heat capacity functions were analyzed by fitting the data to the two-state irreversible model according to (3). On applying this analysis on the two observed transitions, the parameters presented in Table 1 were obtained. Apparently a small part of the β-HpH molecule (corresponding to a ΔH contribution of about 35 MJ mol^{-1}) is more stable than the main part (corresponding to a ΔH contribution of about 150 MJ mol^{-1}). This part would still retain its native conformation while the other part is already denatured. The activation energy for denaturation, however, is similar for both transitions (about 500 kJ mol^{-1}). It is tempting to correlate the two transitions with the denaturation of, respectively, the wall (constituted of FUs *abcdef*) and collar (constituted of FUs *g* and *h*) of the β-HpH molecule.

3.2. DSC Study of β-HpH Substructures

In order to provide further insight into the thermal unfolding pathway of β-HpH, DSC experiments were performed with the structural subunits and FUs that form the Hc molecule. Thermal denaturation of β-HpH subunits was studied in 130 mM glycine/NaOH buffer, pH 9.6 (buffer B) (Fig. 4). In this medium β-HpH is outside its pH stability region [20] and completely dissociated into subunits as evidenced by analytical ultracentrifugation data [21]. For comparison, the calorimetric profiles of the isolated FUs *d* and *g* were also recorded in the same buffer (pH 9.6). In all cases, the thermal denaturation of the Hc substructures investigated was found to be calorimetrically irreversible. Compared to the didecameric β-HpH, the thermogram of the subunits has a more complex character, with three elementary thermal transitions (close to 72, 78

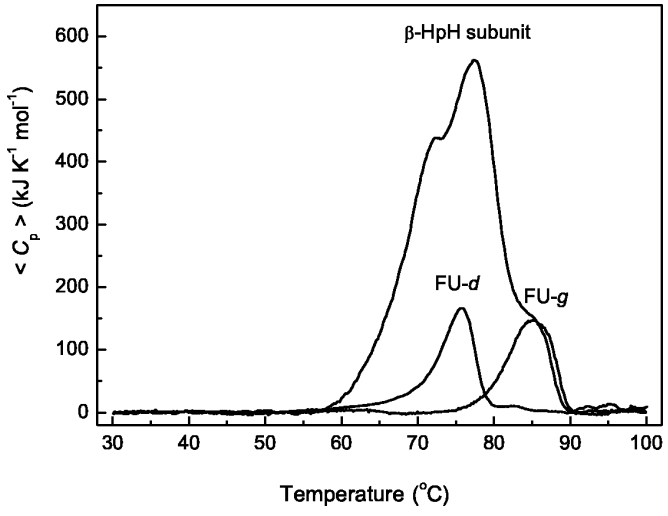

Fig. 4. Calorimetric profiles of β-HpH subunits (6.6 mg ml^{-1}), FU *d* (2.94 mg ml^{-1}) and FU *g* (3.42 mg ml^{-1}) in buffer B at a heating rate of 1.0 K min^{-1}.

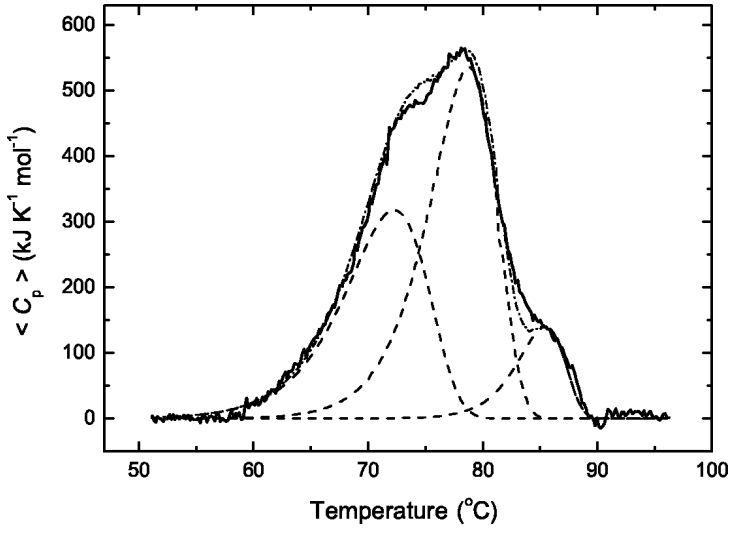

Fig. 5. Result of the successive annealing procedure applied for the experimental deconvolution of the heat capacity curve of β-HpH subunits, which provides three elementary contours (dashed and dashed-dottet lines).

and 85 °C at a scan rate of 1 K min^{-1}). The successive annealing procedure described above was applied for the experimental deconvolution of the thermogram of the β-HpH subunits. Figure 5 shows the final results of this procedure (dashed and continuous lines), which provides three irreversible transitions. The kinetic parameters obtained from the fitting of the experimental data to the two-state irreversible model (3) are presented in Table 2.

Additionally, the FUs investigated showed a single cooperative transition with an apparent T_m at a scan rate of 1 K min^{-1} of ca. 76 °C for FU *d* and of ca. 85 °C for FU *g* (Fig. 4). The heterogeneous profile of the thermogram of the β-HpH subunits can thus be explained in terms of a different stability of the FUs that constitute the subunits. Also, for the FUs of *Rapana thomasiana* hemocyanin structural subunit 2 (RtH2) a

Table 2. Arrhenius equation parameter estimates for the two-state irreversible model of the thermal denaturation of β-HpH subunit at pH 9.6. Scan rate was 1 K min^{-1}.

Transition	Parameter	Value
First	ΔH, MJ mol^{-1}	3.03 ± 0.05
	T^*, °C	76.6 ± 0.2
	E_A, kJ mol^{-1}	276 ± 6
Second	ΔH, MJ mol^{-1}	4.14 ± 0.16
	T^*, °C	82.1 ± 0.2
	E_A, kJ mol^{-1}	357 ± 10
Third	ΔH, MJ mol^{-1}	0.77 ± 0.05
	T^*, °C	87.0 ± 0.3
	E_A, kJ mol^{-1}	521 ± 20

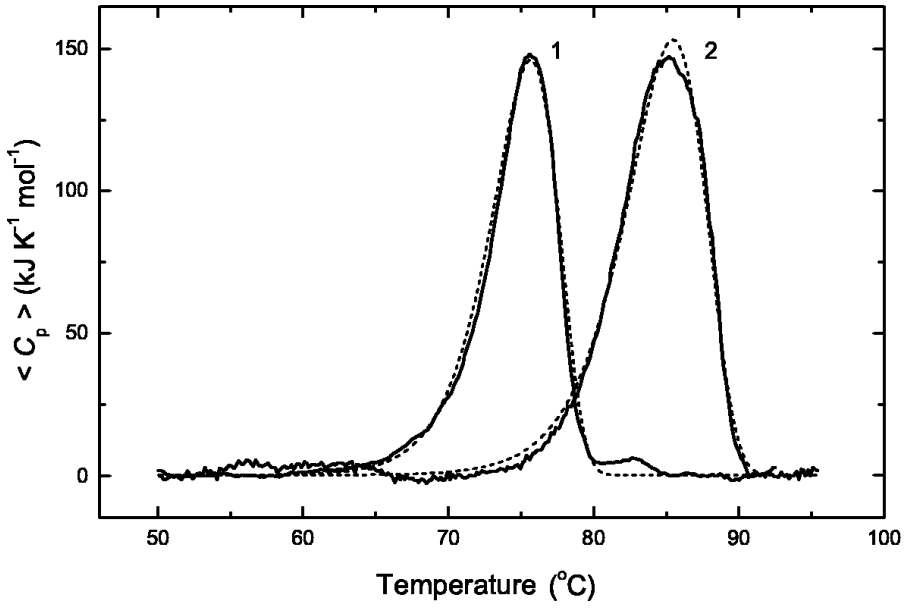

Fig. 6. Calorimetric profiles (solid lines) of FU *d* (line 1) and FU *g* (line 2) in buffer B at a heating rate of 1.0 K min^{-1}. Dashed lines correspond to the fitting of experimental data to the two-state irreversible model [according to (3)].

Table 3. Arrhenius equation parameter estimates for the two-state irreversible model of the thermal denaturation of functional units of β-HpH at pH 9.6. Scan rate was 1 K min^{-1}.

Functional unit	Parameter	Value
	ΔH, kJ mol^{-1}	907 ± 17
d	T^*, °C	77.7 ± 0.2
	E_A, kJ mol^{-1}	437 ± 11
	ΔH, kJ mol^{-1}	1122 ± 19
g	T^*, °C	88.3 ± 0.2
	E_A, kJ mol^{-1}	391 ± 10

difference in thermostability has been observed [31]. Upon comparing the calorimetric profiles of β-HpH subunits and FUs, shown in Fig. 4, the part with a T_m of ca. 85 °C can be identified as corresponding to the FU *g*.

The excess heat capacity functions obtained for FUs *d* and *g* were analyzed by fitting the data to the two-state irreversible model. Figure 6 shows that the theoretical curves (dashed lines) coincide well with the experimental ones (solid lines). Table 3 presents the Arrhenius equation parameters estimated by fitting the experimental data to (3).

When the DSC measurements with FUs *d* and *g* were performed in buffer A, the T_m values shifted to higher temperatures, implying a higher thermostability in this medium (T_m of ca. 86 and 89 °C for FU *d* and *g*, respectively). The increase in stability on turning to the pH 7.2 buffer was larger for FU *d* than for FU *g*. Also, for FU *d* an increase in the ΔH_{cal} value was observed, which could be an indication of association. In the cylindrical structure of gastropodan Hc, FUs *d* and *g* occupy different positions: FU *d* is located in the wall and FU *g*, together with FU *h*, in the collar. From our results, it may be concluded that in β-HpH the FU *g* is the most stable, possibly because it is the richest in carbohydrates among the different FUs [21]. The other collar FU, namely FU *h*, is comparably stable in RtH, as indicated by DSC measurements on the FU RtH1-*h* from subunit 1 of *Rapana thomasiana* Hc [32]. FU *h* plays a key role in the formation of the Hc quaternary structure because it is responsible for the association of two subunits in a dimer. For FU *h* of β-HpH, it has been shown that it occurs as a dimer, even at elevated pH values [21]. This dimerization could be linked to increased thermostability.

4. Conclusions

The results of the present investigation on β-Hc from the gastropodan mollusc *Helix pomatia* allow to classify this Hc as a very thermostable protein.

Differences in stability between the different FUs, as demonstrated for a wall FU (*d*) and a collar FU (*g*), lie at the origin of the complex thermograms observed for the subunits at pH 9.6. As for the didecamers only two transitions (a major and a minor one) were observed at pH 7.2, in contrast to the subunits at pH 9.6 (which show three transitions in a broader temperature region), it is suggested that the FUs in the wall

stabilize each other by associating interactions with their neighbours when assembled into the cylindrical quaternary structure. As a result, at pH 7.2 the wall FUs would denature more or less simultaneously (main transition), while the collar FUs (*g* and *h*) would still keep their native conformation and undergo denaturation at a slightly higher temperature (second and minor transition at pH 7.2).

The high degree of oligomerization of gastropodan hemocyanin molecules in general is probably one of the reasons for the increased thermostability of these dioxygen-binding proteins.

Acknowledgements

We wish to thank the Fund for Scientific Research, Flanders (Belgium) and the Bulgarian Academy of Sciences for financial support for the joint research project "Conformational stability, antigenicity and enzymatic properties of gastropodan hemocyanins". We are grateful to the Katholieke Universiteit Leuven (Belgium) for an IRO fellowship (to N.I.S.). This work was also supported by the research grant TK-X-1611 from the NSF of the Ministry of Education and Science, Bulgaria.

[1] E. F. J. van Bruggen, W. G. Schutter, J. F. L. van Breemen, M. M. C. Bijlholt, and T. Wichertjes, in: Electron Microscopy of Proteins, Vol. I (Ed. J. R. Harris), Academic Press, London, New York 1981, p. 1.
[2] G. Préaux and C. Gielens, in: Copper Proteins and Copper Enzymes, Vol. II (Ed. R. Lontie), CRC Press, Boca Raton, FL 1984, p. 159.
[3] K. E. van Holde and K. I. Miller, Adv. Prot. Chem. **47**, 1 (1995).
[4] M. Guzman-Casado, A. Parody-Morreale, P. L. Mateo, and J. M. Sanchez-Ruiz, Eur. J. Biochem. **188**, 181 (1990).
[5] R. Sterner, T. Vogl, H.-J. Hinz, F. Penz, R. Hoff, R. Föll, and H. Decker, FEBS Lett. **364**, 9 (1995).
[6] D. N. Georgieva, S. Stoeva, S. Ali, A. Abbasi, N. Genov, and W. Voelter, Spectrochim. Acta A **54**, 765 (1998).
[7] K. Idakieva, K. Parvanova, and S. Todinova, BBA **1748**, 50 (2005).
[8] R. Lontie, Life Chem. Rep. Suppl. **1**, 109 (1983).
[9] K. Idakieva, N. I. Siddiqui, K. Parvanova, P. Nikolov, and C. Gielens, BBA **1764**, 807 (2006).
[10] C. Gielens, L. J. Verschueren, G. Préaux, and R. Lontie, in: Invertebrate Oxygen Binding Proteins: Structure, Active Site, and Function (Eds. J. Lamy and J. Lamy), Marcel Dekker, New York 1981, p. 295.
[11] R. Drexel, S. Siegmund, H.-J. Schneider, B. Linzen, C. Gielens, G. Préaux, R. Lontie, J. Kellermann, and F. Lottspeich, Hoppe-Seyler's Z. Physiol. Chem. **368**, 617 (1987).
[12] X.-Q. Xin, C. Gielens, R. Witters, and G. Préaux, in: Invertebrate Dioxygen Carriers (Eds. G. Préaux and R. Lontie), Leuven University Press, Leuven 1990, p. 113.
[13] P. L. Privalov, Adv. Prot. Chem. **35**, 1 (1982).
[14] P. L. Privalov, Annu. Rev. Biophys. Biophys. Chem. **18**, 47 (1989).
[15] A. M. Klibanov and T. J. Ahern, in: Protein Engineering. Thermal Stability of Proteins (Eds. D. L. Oxender and C. F. Fox), Alan R. Liss, New York 1987, p. 213.
[16] J. M. Sanchez-Ruiz, J. L. Lopez-Lacomba, M. Cortijo, and P. L. Mateo, Biochemistry **27**, 1648 (1988).
[17] J. R. Lepock, K. P. Richie, M. C. Kolios, A. M. Rodahl, K. A. Heinz, and J. Kruuv, Biochemistry **31**, 12706 (1992).
[18] V. Shnyrov and G. Zhadan, Recent Res. Devel. Phys. Chem. **4**, 351 (2000).
[19] A. E. Lyubarev and B. I. Kurganov, J. Therm. Anal. Cal. **62**, 51 (2000).
[20] R. Witters and R. Lontie, in: Physiology and Biochemistry of Haemocyanins (Ed. F. Ghiretti), Academic Press, London, New York 1968, p. 61.
[21] E. J. Wood, M. F. Chaplin, C. Gielens, J. De Sadeleer, G. Préaux, and R. Lontie, Comp. Biochem. Physiol. **82B**, 179 (1985).
[22] K. Takahashi and J. M. Sturtevant, Biochemistry **20**, 6185 (1981).
[23] B. I. Kurganov, A. E. Lyubarev, J. M. Sanchez-Ruiz, and V. L. Shnyrov, Biophys. Chem. **69**, 125 (1997).
[24] R. Lumry and H. Eyring, J. Phys. Chem. **58**, 110 (1954).
[25] H. Fukada, J. M. Sturtevant, and F. A. Quiocho, J. Biol. Chem. **258**, 13193 (1983).
[26] V. Edge, N. M. Allewell, and J. M. Sturtevant, Biochemistry **24**, 5899 (1985).
[27] J. M. Sanchez-Ruiz, Biophys. J. **61**, 921 (1992).
[28] S. P. Manly, K. S. Matthews, and J. M. Sturtevant, Biochemistry **24**, 3842 (1985).
[29] V. Shnyrov, G. Zhadan, and I. Akoev, Bioelectromagnetics **5**, 411 (1984).
[30] V. Shnyrov and P. Mateo, FEBS Lett. **324**, 237 (1993).
[31] K. Parvanova, K. Idakieva, S. Stoeva, N. Genov, and W. Voelter, Spectrochim. Acta A **56**, 615 (2000).
[32] K. Parvanova, K. Idakieva, S. Todinova, and N. Genov, BBA **1651**, 153 (2003).